Polymer Chemistry

Accepted Manuscript

ROYAL SOCIETY OF CHEMISTRY

www.rsc.org/polymers

Polymer Chemistry

Polymer Chemistry

Dynamic Article Links ►

Cite this: DOI: 10.1039/c0xx00000x

www.rsc.org/xxxxxx

ARTICLE TYPE

Redox-responsive core cross-linked micelles based on cypate and cisplatin prodrugs-conjugated block copolymers for synergistic photothermal-chemotherapy of cancer

Yu Han,[a] Junjie Li,[a] Minghui Zan,[b] Shizhong Luo,[b] Zhishen Ge*[a] and Shiyong Liu[a]

Received (in XXX, XXX) Xth XXXXXXXXX 20XX, Accepted Xth XXXXXXXXX 20XX
DOI: 10.1039/b000000x

Responsive cross-linked block copolymer micelles which have emerged as promising drug delivery systems showed high stability and on-demand drug release. The combination therapy of cancer can be achieved via co-delivery of varying therapeutic molecules in one system. Here, we developed a redox-responsive core cross-linked (CCL) micelle conjugated by cypate and cisplatin prodrugs within the cores for synergistic photothermal and chemotherapy. The block copolymers, poly[2-(2-methoxyethoxy)ethyl methacrylate)-*co*-(*N*-methacryloxy succinimide)]-*block*-poly(*N*-(2-hydroxypropyl) methacrylamide) (P(MEO_2MA-*co*-MASI)-*b*-PHPMA), were synthesized via reversible addition-fragment chain transfer (RAFT) polymerization. After partial amidation reaction of succinimide with 3-azidopropylamine, the alkynyl-functionalized cypate and Pt(IV) complex were conjugated via click reaction. The CCL micelles were fabricated by core cross-linking at 37 ^{o}C in aqueous solution using cystamine as the cross-linker. P(Pt-Cy-MEO_2MA)-*b*-PHPMA CCL micelles showed redox-responsive cross-linker cleavage and cisplatin drug release in the presence of reductants. The conjugated cypate moieties in the cores of CCL micelles resulted in photothermal temperature increase and reactive oxygen species (ROS) generation under an 805 nm near infrared (NIR) laser irradiation. The cytotoxicity of the CCL micelles was investigated with and without NIR irradiation. Significant synergistic effect of photothermal therapy and chemotherapy was demonstrated against cisplatin-resistant human lung cancer cells A549R under NIR irradiation.

Introduction

Polymeric micelles assembled from amphiphilic block copolymers have been extensively investigated as high-efficiency nanocarriers, especially in cancer diagnosis and therapy.[1-11] In the past decade, various multifunctional micellar delivery vehicles capable of targeting and controlled release of therapeutic agents have been developed. Polymeric micelles utilized as delivery vehicles can provide various advantages including optimizing pharmaceutical and pharmacological behaviors of drugs, prolonging blood circulation duration, overcoming multidrug resistance (MDR) of cancer cells, as well as co-delivery of multiple therapeutic drugs and imaging agents over the same vehicles.[1,5,7,12-15]

It should be noted that there exist the thermodynamic equilibrium between micelles and unimers in aqueous solution, exhibiting disassembly in the dilute solution below their critical micelle concentration (CMC) (e.g. injection into blood circulation).[16-18] To further improve the micellar stability, shell/core cross-linking (SCL/CCL) of the micelles was frequently conducted to prevent premature drug leakage or micellar disintegration.[19-22] The stable CCL or SCL micelles with on-demand stimuli-responsive drug release properties have been explored to deliver various anti-cancer drugs, imaging agents, and co-delivery of different drugs or imaging agents. However, high stability and cross-linked nature of SCL/CCL micelles inevitably hinder the drug release in the targeting sites. To overcome this issue, stimuli-responsive degradable cross-linkers were integrated to prepare CCL or SCL micelles in response to various stimuli including pH, redox, enzyme, light, et al.[7,16-20,23-33] Notably, a significant redox potential difference exists between extracellular space and reducing intracellular environment. Much higher concentration of glutathione (GSH) (~ 10 mM) inside cells determines the reduced microenvironment in cytoplasm.[34] Thus, various redox-responsive polymeric nanocarriers were designed for on-demand and responsive drug release or imaging inside cells. Among them, CCL or SCL micelles on the basis of redox-responsive reversible disulfide bonds were frequently fabricated for higher stability in blood circulation and intracellular reduction-responsive drug release.[7,17,23,27]

On the other hand, photothermal therapy based on near-infrared (NIR) probes attracted great attention in recent years due to their dual-functionality including optical imaging and photothermal therapy.[35-39] The block copolymer micelles were utilized to deliver these molecules for targeting specificity, high stability of the dyes, and long circulation time. Notably, the thermal-chemotherapy on the basis of gold nanorods or magnetic

Fe_3O_4 nanoparticles loading anti-cancer drugs was demonstrated to exhibit synergistic effect, which showed highly efficient cancer cells killing ability and tumor growth inhibition as compared with thermal therapy and chemotherapy alone.[40-43] The reasons for the synergistic effect lied in enhanced drug toxicity in cancer cells that are otherwise resistant to chemotherapeutics upon irradiation probably due to destabilization of subcellular organelles. Moreover, in vivo results also confirmed that the concentration of administrated therapeutic nanoparticles in tumoral region was increased due to increased blood flow and vessel permeability. Taking into account the long-term toxicity of inorganic nanoparticles, the safe organic NIR probes showed significant advantages including high photothermal effect by photoirradiation in the NIR region, facile loading by physical encapsulation or chemical conjugation, low toxicity, and theranostic ability via co-delivery of NIR fluorescent imaging agents and anticancer drugs.[44] However, the literature reports concerning the redox-responsive cross-linked micelles co-delivering anticancer drugs and NIR fluorescent agents for combined photothermal-chemotherapy are relatively rare.

In this report, we fabricated CCL micelles containing cypate moieties and Pt(IV) complex prodrugs for combined photothermal-chemotherapy of cancer (Scheme 1). Firstly, we synthesized diblock copolymer, poly[2-(2-methoxyethoxy)ethyl methacrylate)-*co*-(*N*-methacryloxy succinimide]-*block*-poly(*N*-(2-hydroxypropyl) methacrylamide) (P(MEO_2MA-*co*-MASI)-*b*-PHPMA), via successive reversible addition-fragment transfer (RAFT) polymerization. Then, part of succinimidyl moieties were substituted by 3-azidopropylamine followed by conjugation of cisplatin prodrug and cypate via click reaction. After self-assembly in aqueous solution at 37 °C and core cross-linking by using redox-responsive cross-linker cystamine, the stable CCL micelles were obtained. The redox-responsive disassembly of the CCL micelles in organic solution and the redox-responsive drug release in aqueous solution were investigated. The photothermal temperature increase as a result of generated heat upon NIR irradiation was also studied. Finally, synergistic effect of anti-cancer drug and photothermal toxicity was observed as compared with single photothermal therapy or chemotherapy.

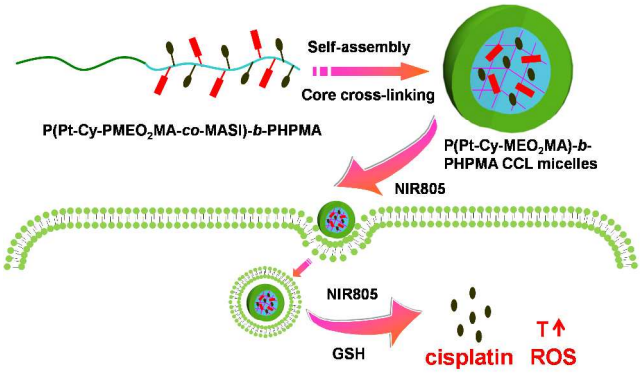

Scheme 1 Schematic illustration of fabrication of CCL micelles via micellization of the block copolymer at 37 °C in aqueous solution and subsequent core cross-linking upon addition of cystamine, and synergistic effect of photothermal and chemotherapy under an 805 nm NIR irradiation in the reductive environment inside cells.

Experimental section

Materials

2-(2-Methoxyethoxy)ethyl methacrylate (MEO_2MA, Aldrich), was vacuum-distilled over CaH_2 and stored at -20 °C prior to use. Copper(I) bromide (CuBr, 99%), *N*,*N*,*N*′,*N*″,*N*″-pentamethyldiethylenetriamine (PMDETA, 98%) 3-chloropropylamine hydrochloride, cisplatin, and 3-azidopropylaminewere purchased from Sigma-Aldrich and used as received. *N*-Hydroxysuccinimide (NHS, 97%, Aldrich) was recrystallized from toluene prior to use. 2,2′-Azobisisobutyronitrile (AIBN, 98%, Fluka) was recrystallized from 95% ethanol. Tetrahydrofuran (THF), 1,4-dioxane, *N*,*N*-dimethylmethanamide (DMF), dichloromethane (DCM), and dimethyl sulfoxide (DMSO) were dried and distilled prior to use. 2-Propynylamine (98%), *N*-(3-dimethylaminopropyl)-*N*′-ethylcarbodiimide hydrochloride (EDC·HCl, 98.5%), 1-hydroxybenzotriazole (HOBT, 97%), propidium iodide (PI, 94%), 1,3-diphenylisobenzofuran (DPBF, 97%), and 4-dimethylaminopyridine (DMAP, 99%) were purchased from Aladdin Reagent Company and used as received. Fetal bovine serum (FBS), trypsin, Dulbecco's modified Eagle's medium (DMEM), and RPMI-1640 medium were purchased from GIBCO and used as received. Cell culture lysis buffer, dihydroethidium (DHE), calcein AM, and 3-(4,5-dimethylthiazol-2,5-diphenyltetrazolium bromide (MTT) from Beyotime Institute of Biotechnology. The cisplatin resistant human lung cancer cell line A549R was purchased from Shanghai Fumengjiyin biotechnology (FMGbio) Co. Ltd. The Pt(IV) complex prodrug, *c,c,t*-[$Pt(NH_3)_2Cl_2(OH)(O_2CCH_2CH_2CO_2H)$],[45] *N*-(2-hydroxypropyl) methacrylamide (HPMA),[46] *N*-methacryloxysuccinimide (MASI),[47] 4-cyanopentanoic acid dithiobenoate (CTP),[48] and cypate[49] were synthesized according to established procedures provided in the literatures. All other commercially available solvents and reagents were purchased from Sinopharm Chemical Reagent Co. Ltd. and used as received.

Characterizations

All nuclear magnetic resonance (NMR) spectra were recorded on a Bruker AV300 NMR 300 MHz spectrometer using DMSO-d_6 or $CDCl_3$ as the solvent. Molecular weights (MWs) and MW distributions were determined by gel permeation chromatography (GPC) using two linear Styragel columns PL1110-6100 and an oven temperature of 30 °C. An Agilent 1260 pump and an Agilent G1362A differential refractive index detector were used. The eluent was DMF at a flow rate of 1.0 mL/min. A series of low polydispersity PEG standards were employed for calibration. A commercial spectrometer (ALV/DLS/SLS-5022F) equipped with a multi-tau digital time correlator (ALV5000) and a cylindrical 22 mW UNIPHASE He-Ne laser (λ_0 = 632 nm) as the light source was employed for dynamic laser light scattering (DLS) measurements. Scattered light was collected at a fixed angle of 90° for duration of 10 min. Distribution averages and particle size distributions were computed using cumulants analysis and CONTIN routines. All data were averaged over three measurements. All samples were filtered through 0.45 μm Millipore Acrodisc-12 filters to remove dust prior to use. The UV-vis absorption spectra were acquired on a Unico UV/vis 2802PCS spectrophotometer. Transmission electron microscopy

(TEM) observations were conducted on a Hitachi H-800 electron

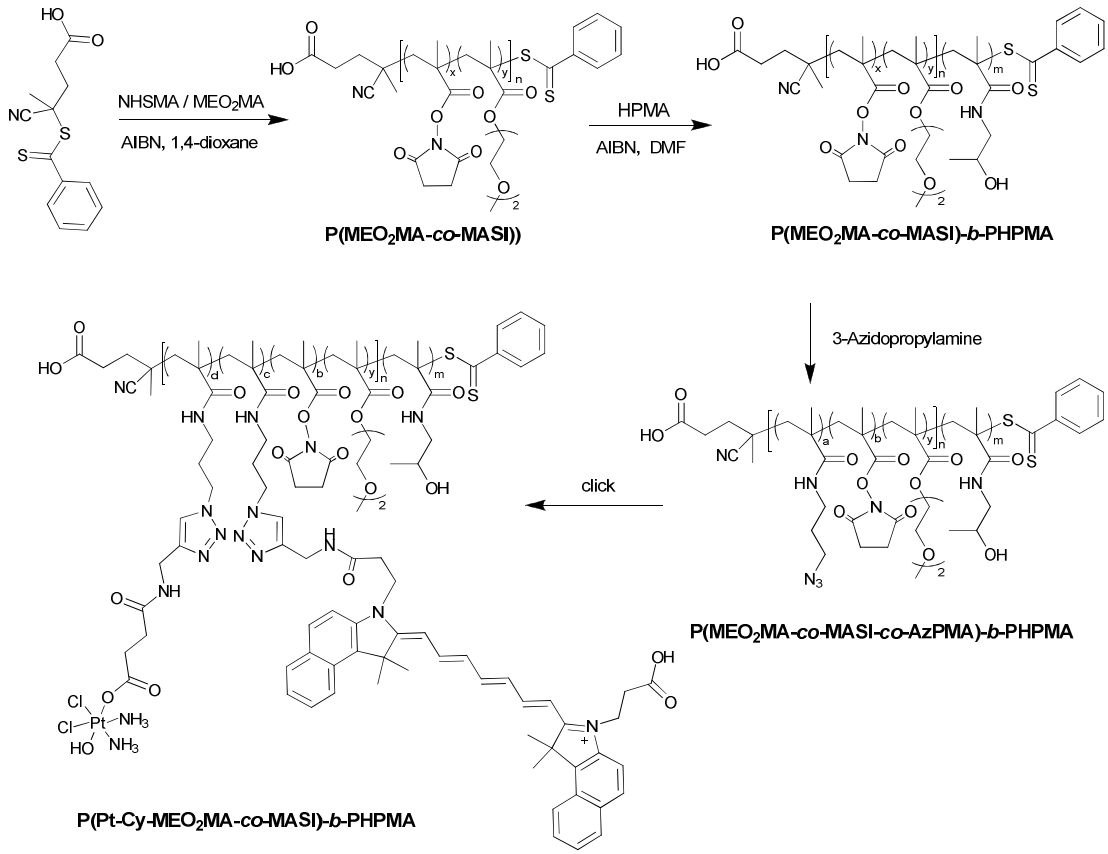

Scheme 2 Synthetic routes employed for preparation of well-defined block copolymer, P(Pt-Cy-*co*-MEO_2MA-*co*-NHSMA)-*b*-PHPMA, covalently attached with Pt(IV) complex prodrugs and near-infrared (NIR) fluorescent dye cypate.

microscope at an acceleration voltage of 200 kV. Platinum content was measured on an X Series 2 Inductively Coupled Plasma Mass Spectrometer (ICP-MS, Thermo fisher Scientific). Confocal laser scanning microscopy (CLSM) images were acquired using Leica TCS SP5 microscope. Reversed-phase HPLC (RP-HPLC) analysis was performed on a Shimadzu HPLC system, equipped with a LC-20AP binary pump, a SPD-20A UV-Vis detector, and a Symmetry C18 column. UV-Vis detector was set at 370 nm for data collection and analysis.

Sample preparation

General procedures employed for the preparation of Pt(IV) complex and cypate conjugated block copolymer, P(Pt-Cy-MASI-*co*-MEO_2MA)-*b*-PHPMA, are shown in Scheme 2.

Synthesis of c,c,t-[Pt(NH_3*)*$_2$*Cl*$_2$*(OH)(*$O_2CCH_2CH_2CONH$*-*$CH_2C{\equiv}CH$*)]*. The *alkynyl*-functionalized Pt(IV) complex, *c,c,t*-[$Pt(NH_3)_2Cl_2(OH)(O_2CCH_2CH_2CONHCH_2C{\equiv}CH)$], was synthesized via EDC coupling reaction. Briefly, *c,c,t*-[$Pt(NH_3)_2Cl_2(OH)(O_2CCH_2CH_2CO_2H)$] (3 g, 6.9 mmol) was dissolved in DMSO solution (40 mL) followed by addition of propargylamine (0.57 g, 10 mmol) and DMAP (0.19 g, 1.6 mmol). After the mixture was cooled to 0 ^oC, EDC·HCl (1.92 g, 10 mmol) was added. The mixture was warmed to ambient temperature over several hours and allowed to stir for 24 h. The solution was then lyophilized and 100 ml acetone was added to precipitate. It was washed with acetone and diethyl ether, dried in a vacuum oven to afford pale yellow solid (2.8 g, 86.0%).^{1}H NMR (δ, ppm, DMSO-d_6): 6.0 (6H, -NH_3), 4.1(2H, -CH_2C≡CH), 2.45-2.25 (4H, -CH_2CH_2-); ESI-MS Calcd. for $(C_7H_{15}Cl_2N_3O_4Pt + H)^+$: 472.2; Found: 472.9; elemental analysis calcd. (%) for $C_7H_{15}Cl_2N_3O_4Pt$: C 17.84, H 3.21, N 8.92; Found: C 18.01, H 3.34, N 8.84. RP-HPLC analysis: elution peak at 7.05 min (80/20, CH_3OH/H_2O, λ = 370 nm) (Fig. S1).

Synthesis of alkynyl-Cypate. Briefly, cypate (3.3 g, 5 mmol) was dissolved in DMF (50 mL) and cooled to 4 ^oC followed by addition of EDC·HCl (1.43 g, 7.5 mmol). After 20 min, HOBt (1.01 g, 7.5 mmol) and propargylamine (0.41 g, 7.5 mmol) were added. The mixture was stirred at room temperature for 24 h and concentrated under vacuum. The residue was dissolved in DCM (100 mL), washed with HCl solution and brine, and dried over $MgSO_4$. The solvents were removed at reduced pressure and purified by flash column chromatography using dichloromethane/methanol (100:5 v/v) as the eluent. After removal of the solvent, the final product was obtained as a green solid (3.1 g, yield: 88.7%). ^{1}H NMR (δ, ppm, DMSO-d_6): 8.5-7.4 (12H, *H* on benz[e]indole), 6.6-6.4 (7H, -C*H*=C*H*-C*H*=C*H*-C*H*=C*H*-C*H*=), 4.4 (4H, -CH_2CH_2CO), 3.8 (2H, -CH_2C≡CH), 2.7-2.8 (4H, -CH_2CH_2CO), 1.8-2.0 (12H, -CH_3) (Fig. S2); ESI-MS Calcd. for $(C_{44}H_{44}O_3N_3Cl + H)^+$: 699.28; Found: 698.6; elemental analysis calcd. (%) for $C_{44}H_{44}O_3N_3Cl$: C 75.68, H 6.35,

N 6.02; Found: C 76.01, H 6.99, N 5.89.

Synthesis of P(MEO_2MA-co-MASI) macroRAFT agent. P(MEO_2MA-*co*-MASI) was prepared by RAFT polymerization of MEO_2MA and MASI using CTP as the chain transfer agent (CTA). To a Schlenk tube equipped with a magnetic stirring bar, the CTP (33 mg, 1.2×10^{-4} mol), AIBN (2.4 mg, 1.5×10^{-5} mol), MEO_2MA (2 g, 10.6 mmol), MASI (1.82 g, 10.6 mmol), and 1,4-dioxane (5 mL) were added. The reaction tube was carefully degassed by three freeze–pump–thaw cycles, sealed under vacuum, and placed in an oil bath thermostated at 70 °C. After 12 h, the tube was broken. The mixture was precipitated into an excess of anhydrous diethyl ether. The above dissolution-precipitation cycle was repeated twice. The final product was dried in a vacuum oven, yielding a pink-red and viscous solid (3.13 g, yield: 81.3%; $M_{n,GPC}$ = 25.9 kDa, M_w/M_n = 1.17) (Fig. 1a). The actual degrees of polymerization (DPs) of MEO_2MA and MASI segments were determined to be 67 and 52, respectively, by ^{1}H NMR analysis in $CDCl_3$ (Fig. S3a). Thus, the polymer was denoted as PMEO_2MA_{67}-*co*-P$MASI_{52}$.

Synthesis of P(MEO_2MA-co-MASI)-b-PHPMA block copolymer. Block copolymer, P(MEOMA-*co*-MASI)-*b*-PHPMA, was prepared by RAFT polymerization of HPMA using P(MEO_2MA-*co*-MASI) as the macroRAFT CAT. To a Schlenk tube equipped with a magnetic stirring bar, PMEO_2MA-*co*-PMASI (1.09 g, 5×10^{-5} mol), AIBN (1 mg, 6.25×10^{-6} mol), HPMA (1.43 g, 10 mmol), and DMF (4 mL) were added. The reaction tube was carefully degassed by three freeze-pump-thaw cycles, sealed under vacuum, and placed in an oil bath thermostated at 80°C. After 16 h, the tube was broken. The mixture was precipitated into an excess of anhydrous diethyl ether. The above dissolution-precipitation cycle was repeated twice. The final product was dried in a vacuum oven, yielding a white solid (1.68 g, yield: 66.6 %; $M_{n,GPC}$ = 47.8 kDa, M_w/M_n = 1.30) (Fig. 1b). The actual DP of HPMA segment was determined to be 148 by ^{1}H NMR analysis in DMSO-d_6 (Fig. S3b). Thus, the polymer was denoted as P(MEO_2MA_{67}-*co*-$MASI_{52}$)-*b*-P$HPMA_{148}$.

Synthesis of P(MEO_2MA-co-MASI-co-AzPMA)-b-PHPMA block copolymer. Block copolymer, P(MEO_2MA-*co*-MASI-*co*-AzPMA)-*b*-PHPMA, was synthesized via amidation reaction between functional activated ester groups and 3-azidopropylamine. Briefly, to a solution of P(MEO_2MA_{67}-*co*-$MASI_{52}$)-*b*-P$HPMA_{148}$ (0.6 g, 1.4×10^{-5} mol) in DMF (2mL), 3-azidopropylamine (36.3 mg, 3.6×10^{-4} mol) in DMF (1 mL) was added dropwise and the reaction mixture was stirred at room temperature for 24 h. The mixture was precipitated into an excess of anhydrous diethyl ether. The above dissolution-precipitation cycle was repeated twice. The final product was dried in a vacuum oven, yielding a white solid (0.51 g, yield: 85.6%). The actual number of PAzPMA segment was determined to be 21 by ^{1}H NMR analysis in DMSO-d_6 (Fig. S3c). Thus, the polymer was denoted as P(MEO_2MA_{67}-*co*-$MASI_{31}$-*co*-$AzPMA_{21}$)-*b*-P$HPMA_{148}$.

Synthesis of Pt(IV) complex and cypate-conjugated block copolymer, P(Pt-Cy-MEO_2MA-co-MASI)-b-PHPMA. The Pt(IV) complex and cypate-conjugated block copolymer, P(Pt-Cy-MEO_2MA-*co*-MASI)-*b*-PHPMA, was synthesized via click reaction between P(AzPMA-*co*-MEO_2MA-*co*-MASI)-*b*-PHPMA and alkynyl-functionalized cypate and Pt(IV) complex. P(MEO_2MA_{67}-*co*-$MASI_{31}$-*co*-$AzPMA_{21}$)-*b*-P$HPMA_{148}$ (0.3 g, 7.0×10^{-6} mol), PMDETA (8.5 mg, 4.9×10^{-5} mol), *alkynyl*-cypate (34.4 mg, 4.9×10^{-5} mol), *c,c,t*-[Pt$(NH_3)_2Cl_2$(OH)$(O_2CCH_2CH_2CONHCH_2C{\equiv}CH)$] (46.4 mg, 9.8×10^{-5} mol), and anhydrous DMF (3 mL) were charged into a 5-mL Schlenk flask. The mixture was degassed by a freeze-pump-thaw cycle and backfilled with N_2. CuBr (7 mg, 4.9×10^{-5} mol) was introduced as a solid under the protection of N_2. The reaction system was then degassed by three freeze-pump-thaw cycles again and sealed under vacuum. Then, the Schlenk flask was placed in a preheated oil bath at 40 °C. After 24 h, the reaction tube was opened, exposed to air, and diluted with 30 mL CH_3OH. The reaction mixture was then passed through a basic alumina column using the mixture of THF and CH_3OH (4:1, v/v) as the eluent to remove the copper catalyst. After removal of the solvents on a rotary evaporator, the mixture was precipitated into an excess of anhydrous diethyl ether. The above dissolution-precipitation cycle was repeated twice. Then, the mixture was further purified by dialysis against distilled water for three days using a dialysis bag (cellulose membrane, molecular weight, cutoff: 6000 Da). The solution was lyophilized, affording as a green powder (0.29 g, yield: 76.3 %). The conjugation number of *c,c,t*-[Pt$(NH_3)_2Cl_2$(OH)$(O_2CCH_2CH_2CONHCH_2C{\equiv}CH)$] was determined to be 14 by ICP-MS, and that of *alkynyl*-cypate was determined to be 7 by UV-vis analysis in DMSO using cypate as the calibration standard. Thus, the polymer was denoted as P(Pt_{14}-Cy_7-MEO_2MA_{67}-*co*-$MASI_{31}$)-*b*-P$HPMA_{148}$. For comparison, cypate-conjugated block copolymer, P(Cy_{21}-MEO_2MA_{67}-*co*-$MASI_{31}$)-*b*-P$HPMA_{148}$ was also prepared according to similar procedures.

Preparation of CCL micelles

Block copolymer, P(Pt_{14}-Cy_7-MEO_2MA_{67}-*co*-$MASI_{31}$)-*b*-P$HPMA_{148}$ (0.1 g), was firstly dissolved in 2.0 mL DMSO, and then quickly injected into 9 mL deionized water in one shot under vigorous stirring. The colloidal dispersion was further stirred for another 2 h, followed by dialysis (MW cutoff, 6 kDa) against deionized water for 12 h to remove DMSO. During this process, fresh deionized water was replaced approximately every 2 h. The final polymer concentration was fixed at 5.0 mg/ml (20 mL) (20 °C). This micelle was used as uncross-linked (UCL) micelles as control. For the preparation of (Pt_{14}-Cy_7-PMEO_2MA_{67})-*b*-P$HPMA_{148}$ CCL micelles, the aqueous solution (10 mL) of UCL micelles was then heated to 37 °C. After equilibration for 30 min at 37 °C, 2.2 mL of an aqueous solution of cystamine (5.0 mg/ml, pH 9.0) preheated to 37 °C was injected. The mixture was stirred for 6 h at 37 °C. Then the mixture was dialyzed against distilled water for three days using a dialysis bag (MW cutoff, 6 kDa). The aqueous solution of P(Pt_{14}-Cy_7-MEO_2MA_{67})-*b*-P$HPMA_{148}$ CCL micelles was further diluted for subsequent studies. Pt content in P(Pt_{14}-Cy_7-MEO_2MA_{67})-*b*-P$HPMA_{148}$ CCL micelle was determined to be 4.92% by ICP-MS, which approximates to the theoretical value (5.15%). For comparison, P(Cy_{21}-MEO_2MA_{67})-*b*-P$HPMA_{148}$ CCL micelles were also prepared according to similar procedures.

In vitro cisplatin release measurements

Typically, P(Pt_{14}-Cy_7-MEO_2MA_{67})-*b*-$PHPMA_{148}$ CCL micelles were dispersed in PBS (pH = 7.4, 5 mL) and then transferred into a dialysis bag. The dialysis bag was immersed in PBS (50 mL) without or with DTT (5 mM and 10 mM) and incubated at 37 °C (100 r/min). At specified time intervals, 5 mL aliquot of the dialysis medium was withdrawn and the same amount of fresh medium was added. Upon each sampling, 5 mL buffer solution was lyophilized. The Pt content was then measured by ICP-MS.

Temperature investigation under NIR irradiation

A volume of 0.2 mL CCL micelles with various cypate concentrations and PBS were placed into the well of a 96-well plate, respectively, and irradiated with an 805 nm NIR laser at a power density of 1 W/cm^2. The time-dependent temperature increasing of the micelles solutions were recorded by an auto-recording thermometer.

In vitro synergistic effect study of photothermal and chemotherapy

Cisplatin-resistant human lung cancer cells A549R were used for *in vitro* cytotoxicity evaluation of P(Pt_{14}-Cy_7-MEO_2MA_{67})-*b*-$PHPMA_{148}$ CCL micelles based on a MTT assay. Briefly, A549R cells were seeded onto 96-well plates at a density of 1×10^4 cells/well in 100 μL RPMI-1640 medium with 10% FBS at 37 °C with 5% CO_2 humidified atmosphere. After 24 h incubation, the original medium was replaced with fresh culture medium, followed by addition of (Pt_{14}-Cy_7-$PMEO_2MA_{67}$)-*b*-$PHPMA_{148}$ CCL micelles or cisplatin with various concentrations of Pt(IV) complex and incubation for 4 h. Then, after 5 min irradiation with an 805 nm NIR laser at 1 W/cm^2, the cells were incubated for another 24 h. MTT solution (20 μL, 5 mg/mL in PBS buffer) was added to each well and incubated for 4 h reaction. The medium in each well was then removed and 100 μL of DMSO was added to dissolve the internalized purple formazan crystals. The plate was subjected to gentle agitation for 15 min until all the crystals were dissolved. The absorbance at wavelength of 490 nm was recorded by a microplate reader (Thermo Fisher). For comparison, Pt(IV) concentration-dependent cytotoxicities of the CCL micelles without NIR irradiation were also tested by a MTT assay.

To conduct cell viability staining, A549R cells were incubated with P(Pt_{14}-Cy_7-MEO_2MA_{67})-*b*-$PHPMA_{148}$ or P(Cy_{21}-MEO_2MA_{67})-*b*-$PHPMA_{148}$ CCL micelles in 12-well microplates for 4 h. Then, after 5 min irradiation with an 805 nm NIR laser at 1 W/cm^2, the cells were incubated for another 24 h. Each well was rinsed and 2 mL PBS was added. Then, each well was treated with 4 μL calcein AM solution (1 mg/mL in DMSO) and continued to be incubated for half an hour. Subsequently, PBS was removed and 1 mL of PI solution (50% in PBS) was added to each well followed by 5 min incubation. Then, each well was washed twice with PBS. Finally, cells immersed in 2 mL PBS of PBS were taken for fluorescence imaging by using CLSM.

Detection of reactive oxygen species (ROS)

Firstly, ROS generation of P(Pt-Cy-MEO_2MA)-*b*-PHPMA CCL micelle solutions was measured in situ by using DPBF, a sensitive probe of ROS.[50] Briefly, the DPBF (15 μM) was mixed with a series of P(Pt_{14}-Cy_7-MEO_2MA_{67})-*b*-$PHPMA_{148}$ CCL micelles solution containing various concentrations of cypate moieties (0 μM, 2.5 μM, 5 μM, 10 μM, 25 μM), respectively. The mixtures were then irradiated with an 805 nm NIR laser at 1 W/cm^2 for 3 min. The fluorescence of DPBF was measured using a spectrometer with the excitation at 405 nm.

ROS production inside the cells was evaluated by a DHE probe known be oxidized by various oxidative agents.[51-52] In brief, A549R cells were seeded into 6-well plate at an initial density of 1×10^5 cells/well in 2 mL of medium with 10% FBS at 37 °C with 5% CO_2 humidified atmosphere. After 24 h incubation, the original medium was replaced with fresh culture medium, followed by addition of P(Pt_{14}-Cy_7-MEO_2MA_{67})-*b*-$PHPMA_{148}$ CCL micelles with cypate moiety concentration of 2.5 μM and subsequent incubation for another 4 h. The medium was replaced with fresh medium, followed by addition of 10 μM DHE. After 30 min incubation, one well was irradiated with 1 W/cm^2 805 nm NIR for 3 min and the other one without irradiation as control. After the medium was removed, the cells were rinsed three times with PBS and observed with fluorescence microscopy.

Intracellular distribution

Intracellular distribution of P(Pt_{14}-Cy_7-MEO_2MA_{67})-*b*-$PHPMA_{148}$ CCL micelles was observed by confocal microscopy. Briefly, A549R cells were seeded onto 35-mm glass-bottom culture dish at a density of 5×10^4 cells/well in 2 mL RPMI-1640 medium with 10% FBS at 37 °C with 5% CO_2 humidified atmosphere. After 24 h incubation, the original medium was replaced with fresh culture medium, followed by addition of P(Pt_{14}-Cy_7-MEO_2MA_{67})-*b*-$PHPMA_{148}$ CCL micelles at the final cypate moiety concentration of 2.5 μM. After 4 h incubation and 5 min irradiation with an 805 nm NIR laser at 1 W/cm^2, the cells were incubated for another 4 h. The medium was removed and the cells were rinsed three times with PBS. Cell nuclei and lysosome were counterstained with DAPI (blue) and Lyso-Tracker (green), respectively. Then, cells were washed three times with cold PBS and observed with CLSM. For comparison, the observation of intracellular distribution of the CCL micelles without irradiation was also carried out under the same conditions.

Results and discussion

Synthesis of block copolymer P(Pt-Cy-MEO_2MA-*co*-MASI)-*b*-PHPMA

RAFT polymerization was frequently used to prepare block copolymers as drug delivery systems due to good control over polymerization of various monomers.[53] In the current work, the block copolymer, P(Pt-Cy-MEO_2MA-*co*-MASI)-*b*-PHPMA, was synthesized via successive RAFT polymerization and subsequent click reaction. The general approach employed for the preparation of P(MEO_2MA-*co*-MASI) macro-RAFT agent, P(MEO_2MA-*co*-MASI)-*b*-PHPMA block copolymer, and the target block copolymer, P(Pt-Cy-MEO_2MA-*co*-MASI)-*b*-PHPMA, were shown in Scheme 2. Firstly, P(MEO_2MA-*co*-MASI) macro-RAFT CAT was prepared via RAFT polymerization of MEO_2MA and MASI in the presence of the RAFT agent CTP. GPC analysis revealed an M_n of 25.9 kDa and a M_w/M_n of 1.17 (Fig. 1a). The DPs of MEO_2MA and PMASI sequences were estimated from the integral ratio of the RAFT agent end group protons with the

chemical shifts at 7.48, 7.57, and 7.84 (b, c, and a) to the methene on NHS moieties (chemical shift 2.88, d) and the methene on the side chains of MEO_2MA groups (chemical shift 3.5-3.9, e) (Fig. S3a). The final DPs of MEO_2MA and MASI in the random copolymer were determined to 67 and 31, respectively. The random copolymer, $P(MEO_2MA_{67}$-*co*-$MASI_{52})$ was subsequently used as macroRAFT agent to control the polymerization of HPMA. The feed ratio of HPMA monomer: macroRAFT agent: initiator ratio that we used was 400:1:0.25. After 18 h polymerization, the conversion of HPMA monomer was 36.5% and the DP of PHPAM was determined to be 148 from ^{1}H NMR analysis (Fig. S3b). GPC analysis of P(MEO_2MA-*co*-MASI)-*b*-PHPMA block copolymer as shown in Fig. 1b revealed a monomodal elution peak and an obvious shift to the higher molecular weight (MW) side as compared with the corresponding macroRAFT agent, P(MEO_2MA-*co*-MASI). On the other hand, no shoulder existed at the elution volume of P(MEO_2MA-*co*-MASI) macro-RAFT agent indicating that no presence of dead P(MEO_2MA-*co*-MASI) CTA in the starting polymerization of HPMA despite a little broad MW distribution (M_w/M_n = 1.31).

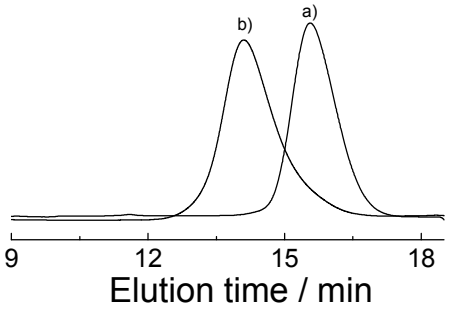

Fig. 1 DMF GPC traces obtained for a) P(MEO_2MA-*co*-MASI) macroRAFT agent (M_n = 25,900, M_w/M_n = 1.17) and b) P(MEO_2MA-*co*-MASI)-*b*-PHPMA block copolymer (M_n = 47,800, M_w/M_n = 1.31).

In order to introduce azide groups in the block copolymer, $P(MEO_2MA_{67}$-*co*-$PMASI_{52})$-*b*-$PHPMA_{148}$, part of oxysuccinimide groups was substituted by 3-azidopropylamine. The presence of azide moieties in P(MEO_2MA-*co*-MASI-*co*-AzPMA)-*b*-PHPMA could be evidently verified by the characteristic infrared absorption peak at ~ 2100 cm^{-1} (Fig. S4a). Moreover, the DPs of PAzPMA sequences can be calculated to be 21 from relative decrease of the pick integration at 3.0 ppm (Fig. S3c). And the final diblock copolymer was denoted as $P(MEO_2MA_{65}$-*co*-$MASI_{31}$-*co*-$AzPMA_{21})$-*b*-$PHPMA_{148}$. The final Pt(IV) complex prodrug and cypate-conjugated block copolymer, P(Pt(IV)-Cy-MEO_2MA-*co*-MASI)-*b*- PHPMA, was prepared by copper(I)-catalyzed alkynyl-azide click reaction which have been demonstrated to an efficient reaction for the synthesis various functionalized polymers.[54] Alkynyl functionalized Pt(IV) complex and cypate, which were both synthesized via EDC condense coupling reaction, were used to attach onto backbone of the block copolymer. A slight excess of *c,c,t*-[$Pt(NH_3)_2Cl_2(OH)(O_2CCH_2CH_2CONHCH_2C{\equiv}CH)$] and alkynyl-cypate with the molar ratio of 1/2 relative to azide moieties was used to react with $P(MEO_2MA_{65}$-*co*-$MASI_{31}$-*co*-$AzPMA_{21})$-*b*-$PHPMA_{148}$ in the presence of CuBr/PMDETA as the catalyst. The ^{1}H NMR spectrum as shown in Fig. S3d revealed that the appearance of signals characteristic of cypate in the range of 6.4-6.7 ppm (b) and 7.5- 8.5 ppm (f) confirming that the successful conjugation of cypate groups. Moreover, the FT-IR spectra shown in Fig. S4b further verified that the quantitative azide groups transformation by the complete disappearance of the characteristic peak of azide moieties at ~ 2100 cm^{-1}. The amount of conjugated Pt(IV) prodrugs and cypate groups can be measured precisely by ICP-MS and UV-vis analysis using cypate as the calibration standard, respectively. The resultant average numbers of Pt(IV) complex and cypate within each block copolymer chain were determined to be 14 and 7, respectively. Thus, the block copolymer was denoted as $P(Pt_{14}$-Cy_7-MEO_2MA_{65}-*co*-$MASI_{31})$-*b*-$PHPMA_{148}$.

Formation of P(Pt-Cy-MEO_2MA)-b-PHPMA CCL micelles

The active ester, NAS, has been explored to be incorporated into block copolymers for shell and core cross-linking (SCL or CCL) to prepare stable SCL or CCL micelles. McCormick et al.[55] and Liu et al.[56] successfully fabricated reduction-responsive SCL and CCL micelles, respectively, from NAS-containing block copolymer using dilsulfide and primary amine-containing cystamine as the reversible cross-linker. In the current work, the NAS residues highly reactive to primary amines were also selected for fabrication of CCL micelles. Firstly, $P(Pt_{14}$-Cy_7-MEO_2MA_{65}-*co*-$MASI_{31})$-*b*-$PHPMA_{148}$ block copolymer micelles were prepared via self-assembly at 20 ^{o}C in aqueous solution. Despite hydrophilic property of MEO_2MA sequences at 20 ^{o}C, relatively high content of hydrophobic NAS and cypate moieties leads to micellization of the block copolymer in aqueous solution. With the temperature increasing to 37 ^{o}C, cores of the micelles became more compact, as revealed by the size decrease of the micelles. In aqueous solutions with the temperatures increasing from 20 ^{o}C to 37 ^{o}C, the average diameters of the micelles decreased from 108 nm to 71 nm due to thermal-responsive properties of $PMEO_2MA$ sequences with lower critical solution temperature (LCST) of ~ 26 ^{o}C.[57]

P(Pt-Cy-MEO_2MA)-*b*-PHPMA CCL micelles were prepared via core cross-linking of $P(Pt_{14}$-Cy_7-MEO_2MA_{65}-*co*-$MASI_{31})$-*b*-$PHPMA_{148}$ micelles by adding 0.7 equiv of cystamine cross-linker relative to the NAS unit in aqueous solution. Six hours after addition of cystamine, CCL micelles were considered to be formed. TEM and DLS were used to characterize the P(Pt-Cy-MEO_2MA)-*b*-PHPMA CCL micelles (Fig. 2a and b). TEM measurements showed spherical morphology of the (Pt-Cy-$PMEO_2MA$)-*b*-PHPMA CCL micelles with the average size of 43 ± 15 nm, which reflected cores of the CCL micelles due to high contras of Pt(IV) prodrugs whereas the hydrophilic shell of the polyplex micelles were not observed due to low contrast in TEM images. DLS analysis revealed P(Pt-Cy-MEO_2MA)-*b*-PHPMA CCL micelles exhibited uniform size with relatively low size distribution μ_2/Γ^2 of 0.114 and relatively small size with $\langle D_h \rangle$ of 68.1 nm in aqueous solution at 37 ^{o}C.

In order to confirm the successful formation of CCL micelles, we evaluated the change of size and scattering intensity for the UCL and CCL micelles upon addition of excess DMF into the micelle solution, a good solvent for all the component of the

micelles (Fig. 3). At 20 °C, the size and scattering intensity of the UCL and CCL micelles were found to be nearly identical in aqueous solution. Upon dilution with 10-fold volume of DMF, UCL micelles were dissociated completely as evidenced by the sharp decrease of light-scattering intensity. Apparently, the micelles solution turned out to be clear from bluish tinge. In contrast, the transmittance of the aqueous solution of the CCL micelles exhibited negligible change, and the light-scattering intensity slightly increased with addition of 10-fold DMF. Moreover, the intensity-average hydrodynamic diameter of the CCL micelles increased from 78.9 nm to 127.4 nm due to the swelling of hydrophobic cores of the CCL micelles. On the other hand, because the CCL micelles were constructed by the reduction-responsive cross-linker, the CCL micelles were expected to be dissociated after treatment with DTT and subsequently added 10-fold DMF. The light-scattering intensity was used to test this process, which showed dramatic decrease after reaction with DDT and subsequent dilution with 10-fold DMF. Thus, these results confirmed the successful fabrication of CCL micelles possessing reduction-responsive properties. Moreover, the stability of CCL micelles in the presence of 10% fetal bovine serum and 150 mM NaCl were also confirmed by DLS. The size of the CCL miclles kept nearly constant, which changed from 68.1 nm to 70.4 nm even after 24 h incubation at 37 °C.

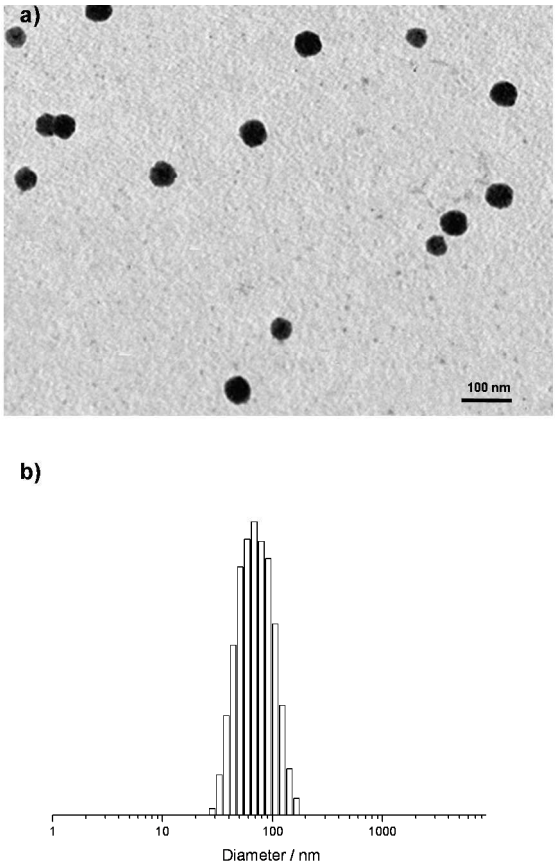

Fig. 2 Characterization of the P(Pt_{14}-Cy_7-MEO_2MA_{67})-*b*-$PHPMA_{148}$ CCL micelles in aqueous solution at 37 °C at the concentration of 1 mg/mL. (a) TEM morphologies and (b) size measurements.

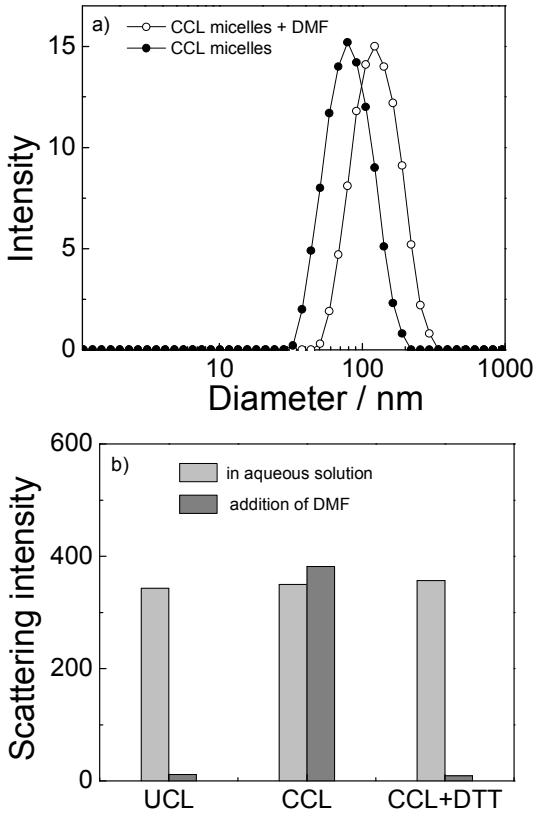

Fig. 3 DLS characterization of micelles (a) swelling of P(Pt_{14}-Cy_7-MEO_2MA_{67})-*b*-$PHPMA_{148}$ CCL micelles upon dilution by 10-fold volume of DMF, (b) laser light scattering intensity of uncross-linked micelles (UCL) in DMF, CCL micelles in DMF (CCL), and CCL micelles in DMF before and after treatment with 10 mM DTT (CCL + DTT) at 20 °C.

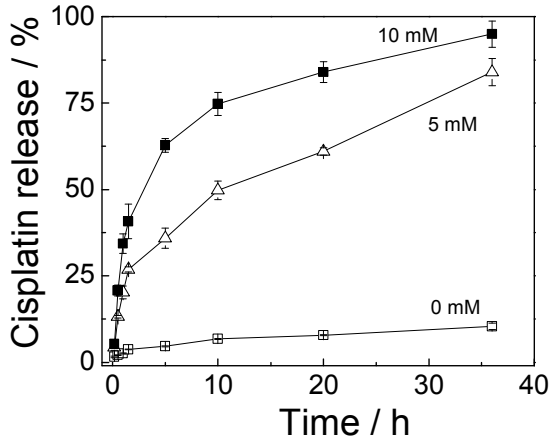

Fig. 4 Cisplatin release profiles of P(Pt_{14}-Cy_7-MEO_2MA_{67})-*b*-$PHPMA_{148}$ CCL micelles in PBS at pH 7.4 and 37 °C in the presence of various concentrations of DTT (0 mM, 5 mM, and 10 mM). Data are expressed as mean ± SD, n = 3.

In vitro drug release and photothermal effect

The Pt(IV) prodrugs can be reduced to active anticancer Pt(II) drug cisplatin under intracellular reductive environment. Thus, various drug delivery systems were investigated to deliver Pt(IV) prodrug species into cells.[58-61] In the current work, firstly, we investigated the reduction-responsive transformation of alkynyl

functionalized Pt(IV) complex into cisplatin in the presence of DTT using RP-HPLC analysis (Fig. S1). As compared with the pick of cisplatin, the successful reduction of Pt(IV) prodrugs into cisplatin can be confirmed. On the other hand, both the cross-linkers and Pt(IV) prodrugs in P(Pt-Cy-MEO_2MA)-*b*-PHPMA CCL micelles are expected to exhibit reduction-responsive behaviors. We then investigated the cisplatin drug release profiles of P(Pt-Cy-MEO_2MA)-*b*-PHPMA CCL micelles in response to the reduction stimulus. The amount of released cisplatin drug was determined precisely via ICP-MS measurements. Time-dependent accumulative released platinum relative to the total platinum payload in the P(Pt-Cy-MEO_2MA)-*b*-PHPMA CCL micelles was measured in the presence of various concentrations of DTT at 37 ^oC and pH 7.4. Fig. 4 shows that the platinum release profiles of P(Pt-Cy-MEO_2MA)-*b*-PHPMA CCL micelles in the presence of 0, 5, and 10 mM DDT in aqueous solution. After 10 h incubation, upto 74.5% and 49.2% platinum was released in the presence of 5 mM and 10 mM DTT, respectively, while in the absence of DTT, less than 10% platinum was released even after 36 h incubation, which confirmed that the reduction-responsive drug release behaviors. The 8% platinum release in the absence of DTT are presumably attributed to the hydrolysis of the linkage between the Pt(IV) complexes and the polymer backbones. As compared with the previous report where 24% platinum conjugated on the uncross-linked amphiphilic block copolymer micelles was released after incubation of 10 h at pH 7.4,[58] the significantly slow release rate in the current work in the absence of DTT should be ascribed to the high stability of the CCL micelles.

The UV-vis absorption spectra of free cypate and P(Pt-Cy-MEO_2MA)-*b*-PHPMA CCL micelles were further measured. As shown in Fig. 5a, free cypate molecules showed a highest absorption pick at 783 nm. On the other hand, the absorption curves of cypate moieties inside the P(Pt_{14}-Cy_7-MEO_2MA_{67})-*b*-$PHPMA_{148}$ CCL micelles exhibited a red shift with two obvious absorption picks located at 735 nm and 798 nm, respectively. We then evaluated the photothermal effect and temperature increment including PBS and various concentrations of cypate moieties in a series of P(Pt-Cy-MEO_2MA)-*b*-PHPMA CCL micelles under 805 nm laser irradiation at a power density of 1 W/cm^2. PBS as control showed no temperature increase under the NIR irradiation. In contrast, at the CCL micelles containing cypate moiety concentration of 3 μM, the temperature of micelle solution (0.2 mL) increased quickly from 20 ^oC to 42 ^oC within 1 min, and the CCL micelles containing higher cypate moiety concentrations showed more significantly temperature increasing. The results indicated that cypate conjugated in the CCL micelles can effectively generate hyperthermia upon NIR irradiation, which can lead to cell death with the temperature higher than 42 ^oC.[35-36]

Synergistic cytotoxic effects of photothermal and chemotherapy

To evaluate synergistic cytotoxicity of photothermal hyperthermia and chemotherapy of P(Pt-Cy-MEO_2MA)-*b*-PHPMA CCL micelles against cisplatin-resistant human cancer cells A549R, we measured in vitro cytotoxicity of the CCL micelles with and without NIR irradiation at various concentrations of CCL micelles. We incubated A549R cells with CCL micelles at various concentrations for 4 h and then exposed to an 805 nm laser at a power density of 1 W/cm^{-2} for 5 min. Then, the cells were washed three times with PBS to remove drugs and incubated in drug-free medium for 48 h. Subsequently, the cells were stained with calcein AM and PI for live cells (green) and dead cells (red), respectively. As shown in Fig. 6A(a_1), the growth of cells was not affected evidently under only NIR irradiation without addition of CCL micelles. With addition of P(Cy_{21}-MEO_2MA_{67})-*b*-$PHPMA_{148}$ CCL micelles containing cypate moiety concentration of 1.2 μM, a small population of cells were dead under NIR irradiation, as indicative of an extremely small red regions captured with a microscopy due to low temperature increase at this cypate moiety concentration (Fig. 6A(a_2)). However, with cypate moiety concentration increasing to 3 μM, nearly half of cells were dead (Fig. 6A(a_3)). On the other hand, as for P(Pt-Cy-MEO_2MA)-*b*-PHPMA CCL micelles without NIR irradiation, dead cells regions (red) can be observed apparently in the CLSM images at the platinum concentration of 2.4 and 6 μM, respectively (Fig. 6A(b_1 and b_2)). Moreover, upon combined treatment of photothermal and chemotherapy using P(Pt-Cy-MEO_2MA)-*b*-PHPMA CCL micelles upon NIR irradiation, the red regions were enlarged significantly as compared with single photothermal and chemotherapy Fig. 6A(c_1 and c_2). Notably, at cypate moiety concentration of 3 μM within P(Pt-Cy-MEO_2MA)-*b*-PHPMA CCL micelles, nearly 95% cells were dead under NIR irradiation.

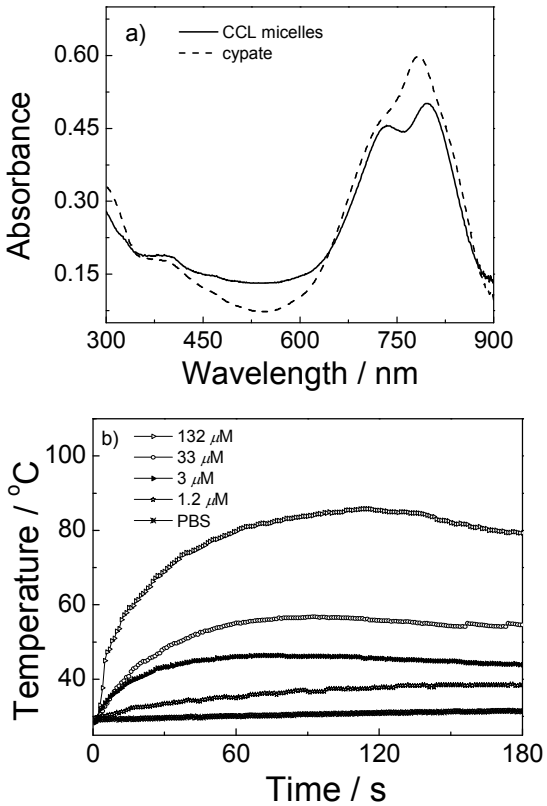

Fig. 5 (a) UV-vis absorbance spectra of free cypate and P(Pt_{14}-Cy_7-MEO_2MA_{67})-*b*-$PHPMA_{148}$ CCL micelles in aqueous solution; (b) Temperature rise profiles of a series of P(Pt_{14}-Cy_7-MEO_2MA_{67})-*b*-$PHPMA_{148}$ CCL micelles containing various concentrations of cypate moieties (1.2, 3, 33, and 132 μM) under an 805 nm NIR laser irradiation at a power density of 1 W/cm^2.

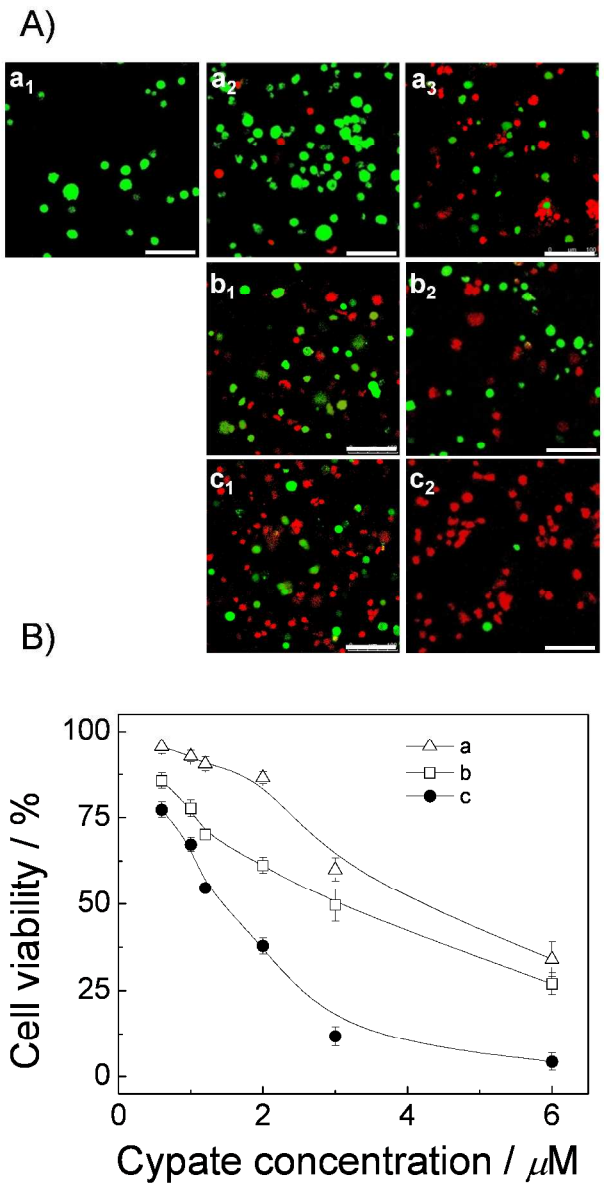

Fig. 6 Cell survival of A549R after treatment using CCL micelles. (A) FL images of A549 cells after treatment using CCL micelles with different concentrations (a_1-a_3: PBS, P(Cy_{21}-MEO_2MA_{67})-*b*-$PHPMA_{148}$ CCL micelles containing 1.2 μM and 3 μM cypate moieties under an 805 nm NIR irradiation at a power density of 1 W/cm^{-2} for 5 min; b_1, b_2: P(Pt_{14}-Cy_7-MEO_2MA_{67})-*b*-$PHPMA_{148}$ CCL micelles containing Pt(IV) prodrug 2.4 μM and 6 μM without NIR irradiation; c_1, c_2: P(Pt_{14}-Cy_7-MEO_2MA_{67})-*b*-$PHPMA_{148}$ CCL micelles containing 1.2 μM and 3 μM cypate moieties under an 805 nm NIR irradiation at a power density of 1 W/cm^{-2} for 5 min). Viable cells were stained green with calcein-AM, and dead/later apoptosis cells were stained red with PI. Scale bars represent 100 μm. (B) Cell viability of A549R cells after treatment with CCL micelles (a: P(Cy_{21}-MEO_2MA_{67})-*b*-$PHPMA_{148}$ CCL micelles under an 805 nm NIR irradiation at a power density of 1 W/cm^{-2} for 5 min; b: P(Pt_{14}-Cy_7-MEO_2MA_{67})-*b*-$PHPMA_{148}$ CCL micelles without NIR irradiation; c: P(Pt_{14}-Cy_7-MEO_2MA_{67})-*b*-$PHPMA_{148}$ CCL micelles under an 805 nm NIR irradiation at a power density of 1 W/cm^{-2} for 5 min). Data are expressed as mean ± SD, n = 4.

To determine the synergistic cytotoxic effect of photothermal hyperthermia and chemotherapy quantitatively, we compared the cytotoxic effects of P(Pt-Cy-MEO_2MA)-*b*-PHPMA CCL micelles without laser irradiation (chemotherapy using the Pt(IV) prodrugs), P(Cy-MEO_2MA)-*b*-PHPMA CCL micelles with laser irradiation (photothermal therapy), and P(Pt-Cy-MEO_2MA)-*b*-PHPMA CCL micelles with laser irradiation (combined photothermal and chemotherapy) by MTT assay. A549R cells were exposed to CCL micelles for 4 h with or without subsequent an 805 nm laser irradiation at 1 W/cm^{-2} for 5 min. Then, the cells were washed three times with PBS to remove drugs and incubated in drug-free medium for 24 h followed by MTT assay. Notably, P(Cy-MEO_2MA)-*b*-PHPMA CCL micelles with the cypate groups concentration lower than 8 μM showed negligible cytotoxicity against A549R cells without NIR irradiation, which all exhibited more than 95% cell viability due to the good biocompatibility of the main polymer components ($PMEO_2MA$ and PHPMA) (Fig. S5). Cisplatin drug showed very low cytotoxicity against A549R cells at the cisplatin concentration of lower than 10 μM due to cisplatin drug-resistant properties of A549R cells with high half maximal inhibitory concentration (IC50) values upto 29 μM.[62] CCL micelles exhibited higher cytotoxicity against A549R cells than cisplatin due to a varying drug transportation mechanism into the cells that can overcome drug-resistance of A549R cells.[61] Fig. 6b shows cell viabilities after treatment with P(Cy-MEO_2MA)-*b*-PHPMA CCL micelles with NIR irrdiation, P(Pt-Cy-MEO_2MA)-*b*-PHPMA CCL micelles without laser irradiation, and P(Pt-Cy-MEO_2MA)-*b*-PHPMA CCL micelles under NIR irradiation. The combined photothermal hyperthermia and chemotherapy of P(Pt-Cy-MEO_2MA)-*b*-PHPMA CCL micelles exhibited significantly increased cytotoxicity as compared with single photothermal or chemotherapy especially when the cypate moiety concentration is higher than 1.2 μM. For instance, P(Pt-Cy-MEO_2MA)-*b*-PHPMA CCL micelles with cypate moiety concentration of 3 μM and Pt(IV) 6 μM showed 11.8% cell viability while single photothermal and chemotherapy showed 59.9% and 49.7% cell viability, respectively.

Table 1 The comparison between the additive percentage (p_{add}) and combined percentage (p_{com}) of cell survival upon treatment of photothermal and chemotherapy using CCL micelles with typical cypate moiety concentrations.

cypate moiety concentrations / μM	p_{add} / %	p_{com} / %
1.2	63.44	54.68
2	52.95	37.82
3	29.80	11.77

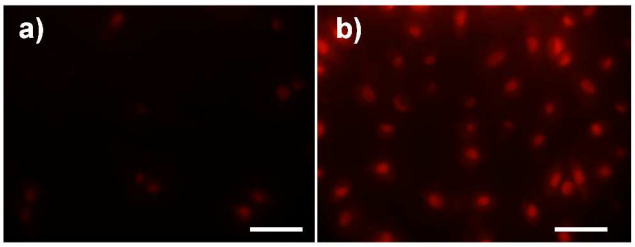

Fig. 7 The fluorescence microscopy images of A549R cells incubated with (a) P(Pt_{14}-Cy_7-MEO_2MA_{67})-*b*-$PHPMA_{148}$ CCL micelles and stained by DHE and (b) P(Pt_{14}-Cy_7-MEO_2MA_{67})-*b*-$PHPMA_{148}$ CCL micelles under an 805 nm NIR laser irradiation at a power density of 1 W/cm^2 and stained with DHE. The concentration of cypate moieties was 2.5 μM. Scale bars represent 50 μm.

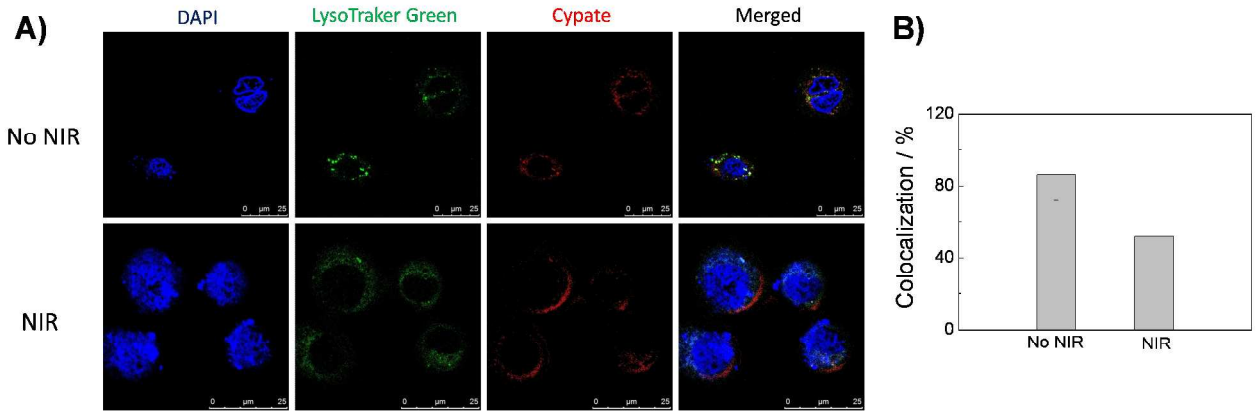

Fig. 8 (A) CLSM observation of the intracellular distribution of P(Pt_{14}-Cy_7-MEO_2MA_{67})-*b*-$PHPMA_{148}$ CCL micelles (red) with late endosome/lysosomes (green) and nuclei (blue) stained with LsoTracker Green and DAPI, respectively, with and without irradiation under an 805 nm NIR laser at 1 W/cm^2 for 3 min. (B) Quantification of colocalizations between P(Pt_{14}-Cy_7-MEO_2MA_{67})-*b*-$PHPMA_{148}$ CCL micelles and LysoTracker Green. Data are expressed as mean ± SD, n = 20.

Moreover, the synergistic effect of the combined treatment of photothermal and chemotherapy can be determined by the additive cell viability which is the percentage of surviving cells by additive interaction of photothermal hyperthermia and chemotherapy (p_{add}).[40,63] It can be calculated by the product of the percentage of surviving cells after photothermal hyperthermia treatment (p_{pho}), and that after chemotherapy (p_{che}) ($p_{add} = p_{pho} \times p_{che}$). Thus, whether the synergistic effect exists can be judged by the comparison between p_{add} and the percentage of surviving cells after combination treatment of photothermal hyperthermia and chemotherapy (p_{com}). When $p_{com} < p_{add}$, a synergistic effect is considered to be existent. Typically, when the cypate moiety concentration of CCL micelles was 1.2, 2.0 and 3.0 μM where the and Pt(IV) concentrations was 2.4, 4.0 and 6.0 μM, respectively, the remarkable synergistic effect existed during combined cancer therapy against A549R cells (Table 1).

Previously, cellular membrane permeability and drug diffusion increase induced by thermal effect have been demonstrated by various gold nanorods drug delivery systems.[40-41] Thus, a synergistic effect between photothermal hyperthermia and chemotherapy resulted in amplifying the therapeutic outcome dramatically. On the other hand, Chen et al.[35] confirmed that cypate molecules could effectively disrupt endo/lysosomal membranes at very low dose of 0.5 μg/mL under the NIR laser irradiation at a power density of 1 W/cm^2. In the current work, we first tested the ROS generation of P(Pt-Cy-MEO_2MA)-*b*-PHPMA CCL micelles under NIR irradiation by using DPBF, which can be quickly oxidized by ROS resulting in degradation of DPBF and reduction of corresponding fluorescence intensity.[50] The relative fluorescence intensity of DPBF was measured in the presence of P(Pt_{14}-Cy_7-MEO_2MA_{67})-*b*-$PHPMA_{148}$ CCL micelles with varying concentrations under an 805 nm NIR laser irradiation at a power density of 1 W/cm^2 for 3 min (Fig. S6). The decrease of relative fluorescence intensity can be observed clearly with the cypate moiety concentrations increasing as indicative of ROS generation. Furthermore, we found that ROS were generated inside cells in the presence of P(Pt-Cy-MEO_2MA)-*b*-PHPMA CCL micelles with NIR irradiation, which were examined by using DHE as the fluorescent probe.[64] As shown in Fig. 7, the A549 cells incubated with P(Pt-Cy-MEO_2MA)-*b*-PHPMA CCL micelles showed significantly higher fluorescent intensity under an 805 nm laser NIR irradiation for 5 min as compared with that without NIR irradiation, indicating that the cypate moieties could also generate ROS inside cells under the excitation of NIR irradiation.

The photothermal effect and ROS both result in cytotoxicity. Meanwhile, they can also trigger the disruption of endo/lysosome, which will enhance the endo/lysosomal escape efficiency of the CCL micelles. To confirm the disruption capability of P(Pt_{14}-Cy_7-MEO_2MA_{67})-*b*-$PHPMA_{148}$ CCL micelles towards endo/lysosome under NIR irradiation, the intracellular distribution of CCL micelles was investigated using CLSM (Fig. 8). The colocalizations between LysoTracker green and the CCL micelles reflect the endo/lysomal escape ability. The CCL micelles under NIR irradiation showed lower colocalization value revealing that higher endo/lysomal disruption and escape capability as compared with that without NIR irradiation. Thus, higher dissociation of CCL micelles and improved therapeutic effect can be achieved following increased reduction rate from Pt(IV) complex to active cisplatin in cytoplasm. Therefore, the synergistic effect of cypate and Pt(IV) prodrug conjugated in the reduction-responsive P(Pt-Cy-MEO_2MA)-*b*-PHPMA CCL micelles could overcome drug-resistance of A549R cells effectively and improve the therapeutic effect significantly under NIR irradiation due to improved temperature, ROS generation, and chemotherapy.

Conclusions

In this work, we successfully fabricated reduction-responsive P(Pt-Cy-MEO_2MA)-*b*-PHPMA CCL micelles conjugated with cypate and Pt(IV) prodrugs via successive RAFT polymerization, subsequent click reaction, and final core cross-linking. The CCL micelles showed reduction-responsive cleavage of cross-linker and release of active anticancer drug cisplatin in the presence of DTT at 37 ^oC in aqueous solution. The cypate molecules showed photothermal and ROS generation effect under NIR irradiation, which not only produced cytotoxicity against A549R cells but

improved the therapeutic effect of anticancer drug cisplatin via enhancement of drug diffusion and endo/lysosomal disruption. The synergistic effect of photothermal and chemotherapy significantly improved the cytotoxicity of CCL micelles at low concentrations. Notably, the high-stability of the CCL micelles can be expected to facilitate the retention in blood circulation which can provide the probability of in vivo practical applications for cancer therapy. Simultaneously, the cypate moieties can serve as fluorescent imaging probes for theranostic applications. The work toward this direction is underway.

Acknowledgements

The financial support from National Natural Scientific Foundation of China (NNSFC) Project (51273188, 81201176), A Foundation for the Author of National Excellent Doctoral Dissertation of PR China (FANEDD) (201224), the Specialized Research Fund for the Doctoral Program of Higher Education (SRFDP) (20123402120022), Anhui Provincial Natural Science Foundation (APNSF) (1208085QB21) is gratefully acknowledged.

Notes and references

[a] *CAS Key Laboratory of Soft Matter Chemistry, Department of Polymer Science and Engineering, University of Science and Technology of China, Hefei, Anhui 230026, China Tel:+81-551-63603670; E-mail: gezs@ustc.edu.cn*

[b] *Key Laboratory of Functional Molecular Solids, Ministry of Education, Anhui Key Laboratory of Molecule-based Materials, College of Chemistry and Materials Science, Anhui Normal University, Wuhu, Anhui, P. R. China.*

† Electronic Supplementary Information (ESI) available: Fig S1-S6. See DOI: 10.1039/b000000x/

1 K. Kataoka, A. Harada and Y. Nagasaki, *Adv. Drug Delivery Rev.*, 2001, **47**, 113-131.
2 S. M. Janib, A. S. Moses and J. A. MacKay, *Adv. Drug Delivery Rev.*, 2010, **62**, 1052-1063.
3 C. J. F. Rijcken, O. Soga, W. E. Hennink and C. F. van Nostrum, *J. Controlled Release*, 2007, **120**, 131-148.
4 H. Wei, S. X. Cheng, X. Z. Zhang and R. X. Zhuo, *Prog. Polym. Sci.*, 2009, **34**, 893-910.
5 C. Oerlemans, W. Bult, M. Bos, G. Storm, J. F. W. Nijsen and W. E. Hennink, *Pharm. Res.*, 2010, **27**, 2569-2589.
6 M. H. Stenzel, *Chem. Commun.*, 2008, 3486-3503.
7 Z. S. Ge and S. Y. Liu, *Chem. Soc. Rev.*, 2013, **42**, 7289-7325.
8 A. Z. Wang, R. Langer and O. C. Farokhzad, *Annual Review of Medicine, Vol 63*, 2012, **63**, 185-198.
9 M. L. Adams, A. Lavasanifar and G. S. Kwon, *J. Pharm. Sci.*, 2003, **92**, 1343-1355.
10 Z. L. Tyrrell, Y. Q. Shen and M. Radosz, *Prog. Polym. Sci.*, 2010, **35**, 1128-1143.
11 C. Deng, Y. J. Jiang, R. Cheng, F. H. Meng and Z. Y. Zhong, *Nano Today*, 2012, **7**, 467-480.
12 X. B. Xiong, A. Falamarzian, S. M. Garg and A. Lavasanifar, *J. Controlled Release*, 2011, **155**, 248-261.
13 F. Mohamed and C. F. van der Walle, *J. Pharm. Sci.*, 2008, **97**, 71-87.
14 X.-Y. Kea, V. W. L. Ng, S.-J. Gao, Y. W. Tong, J. L. Hedrick and Y. Y. Yang, *Biomaterials*, 2014, **35**, 1096-1108.
15 Q. Yin, J. N. Shen, Z. W. Zhang, H. J. Yu and Y. P. Li, *Adv. Drug Delivery Rev.*, 2013, **65**, 1699-1715.
16 J. Q. Fan, F. Zeng, S. Z. Wu and X. D. Wang, *Biomacromolecules*, 2012, **13**, 4126-4137.
17 J. Dai, S. D. Lin, D. Cheng, S. Y. Zou and X. T. Shuai, *Angew. Chem., Int. Ed.*, 2011, **50**, 9404-9408.
18 C. J. Rijcken, C. J. Snel, R. M. Schiffelers, C. F. van Nostrum and W. E. Hennink, *Biomaterials*, 2007, **28**, 5581-5593.
19 R. K. O'Reilly, C. J. Hawker and K. L. Wooley, *Chem. Soc. Rev.*, 2006, **35**, 1068-1083.
20 E. S. Read and S. P. Armes, *Chem. Commun.*, 2007, 3021-3035.
21 X. Z. Jiang, S. Z. Luo, S. P. Armes, W. F. Shi and S. Y. Liu, *Macromolecules*, 2006, **39**, 5987-5994.
22 C. F. van Nostrum, *Soft Matter*, 2011, **7**, 3246-3259.
23 Z. H. Zhang, L. C. Yin, C. L. Tu, Z. Y. Song, Y. F. Zhang, Y. X. Xu, R. Tong, Q. Zhou, J. Ren and J. J. Cheng, *Acs Macro Lett*, 2013, **2**, 40-44.
24 Z. F. Jia, L. J. Wong, T. P. Davis and V. Bulmus, *Biomacromolecules*, 2008, **9**, 3106-3113.
25 S. Cajot, N. Lautram, C. Passirani and C. Jerome, *J. Controlled Release*, 2011, **152**, 30-36.
26 Y. Chan, T. Wong, F. Byrne, M. Kavallaris and V. Bulmus, *Biomacromolecules*, 2008, **9**, 1826-1836.
27 R. R. Wei, L. Cheng, M. Zheng, R. Cheng, F. H. Meng, C. Deng and Z. Y. Zhong, *Biomacromolecules*, 2012, **13**, 2429-2438.
28 S. Binauld and M. H. Stenzel, *Chem. Commun.*, 2013, **49**, 2082-2102.
29 S. Samarajeewa, R. Shrestha, M. Elsabahy, A. Karwa, A. Li, R. P. Zentay, J. G. Kostelc, R. B. Dorshow and K. L. Wooley, *Mol. Pharm.*, 2013, **10**, 1092-1099.
30 X. L. Hu, H. Li, S. Z. Luo, T. Liu, Y. Y. Jiang and S. Y. Liu, *Polym Chem-Uk*, 2013, **4**, 695-706.
31 L. S. Yan, L. X. Yang, H. Y. He, X. L. Hu, Z. G. Xie, Y. B. Huang and X. B. Jing, *Polym Chem-Uk*, 2012, **3**, 1300-1307.
32 K. R. Raghupathi, M. A. Azagarsamy and S. Thayumanavan, *Chem.-Eur. J.*, 2011, **17**, 11752-11760.
33 Y. Zhao, *Macromolecules*, 2012, **45**, 3647-3657.
34 G. Y. Wu, Y. Z. Fang, S. Yang, J. R. Lupton and N. D. Turner, *J. Nutr.*, 2004, **134**, 489-492.
35 H. Yang, H. J. Mao, Z. H. Wan, A. J. Zhu, M. Guo, Y. L. Li, X. M. Li, J. L. Wan, X. L. Yang, X. T. Shuai and H. B. Chen, *Biomaterials*, 2013, **34**, 9124-9133.
36 C. X. Yue, P. Liu, M. B. Zheng, P. F. Zhao, Y. Q. Wang, Y. F. Ma and L. T. Cai, *Biomaterials*, 2013, **34**, 6853-6861.
37 L. Wu, S. Fang, S. Shi, J. Deng, B. Liu and L. Cai, *Biomacromolecules*, 2013, **14** 3027-3033.
38 J. Yu, D. Javier, M. A. Yaseen, N. Nitin, R. Richards-Kortum, B. Anvari and M. S. Wong, *J. Am. Chem. Soc.*, 2010, **132**, 1929-1938.
39 C. L. Peng, Y. H. Shih, P. C. Lee, T. M. H. Hsieh, T. Y. Luo and M. J. Shieh, *Acs Nano*, 2011, **5**, 5594-5607.
40 F. Ren, S. Bhana, D. D. Norman, J. Johnson, L. J. Xu, D. L. Baker, A. L. Parrill and X. H. Huang, *Bioconjugate Chem.*, 2013, **24**, 376-386.
41 J. H. Park, G. von Maltzahn, M. J. Xu, V. Fogal, V. R. Kotamraju, E. Ruoslahti, S. N. Bhatia and M. J. Sailor, *Proc. Natl. Acad. Sci. U. S. A.*, 2010, **107**, 981-986.
42 A. J. Gormley, N. Larson, S. Sadekar, R. Robinson, A. Ray and H. Ghandehari, *Nano Today*, 2012, **7**, 158-167.
43 T. J. Li, C. C. Huang, P. W. Ruan, K. Y. Chuang, K. J. Huang, D. B. Shieh and C. S. Yeh, *Biomaterials*, 2013, **34**, 7873-7883.
44 M. B. Zheng, C. X. Yue, Y. F. Ma, P. Gong, P. F. Zhao, C. F. Zheng, Z. H. Sheng, P. F. Zhang, Z. H. Wang and L. T. Cai, *Acs Nano*, 2013, **7**, 2056-2067.
45 S. Dhar, W. L. Daniel, D. A. Giljohann, C. A. Mirkin and S. J. Lippard, *J. Am. Chem. Soc.*, 2009, **131**, 14652-14653.
46 J. Strohalm and J. Kopecek, *Angew. Makromol. Chem.*, 1978, **70**, 109-118.
47 J. M. Rathfon and G. N. Tew, *Polymer*, 2008, **49**, 1761-1769.
48 Y. Mitsukami, M. S. Donovan, A. B. Lowe and C. L. McCormick, *Macromolecules*, 2001, **34**, 2248-2256.
49 Y. P. Ye, S. Bloch, J. Kao and S. Achilefu, *Bioconjugate Chem.*, 2005, **16**, 51-61.
50 L. Li, J. F. Zhao, N. Won, H. Jin, S. Kim and J. Y. Chen, *Nanoscale Res Lett*, 2012, **7**.
51 H. Y. Ding, H. J. Yu, Y. Dong, R. H. Tian, G. Huang, D. A. Boothman, B. D. Sumer and J. M. Gao, *J. Controlled Release*, 2011, **156**, 276-280.
52 X. J. Jiang, P. C. Lo, S. L. Yeung, W. P. Fong and D. K. P. Ng, *Chem. Commun.*, 2010, **46**, 3188-3190.
53 C. Boyer, V. Bulmus, T. P. Davis, V. Ladmiral, J. Q. Liu and S. Perrier, *Chem. Rev.*, 2009, **109**, 5402-5436.
54 R. K. Iha, K. L. Wooley, A. M. Nystrom, D. J. Burke, M. J. Kade and C. J. Hawker, *Chem. Rev.*, 2009, **109**, 5620-5686.

55 Y. T. Li, B. S. Lokitz, S. P. Armes and C. L. McCormick, *Macromolecules*, 2006, **39**, 2726-2728.

56 J. Y. Zhang, X. Jiang, Y. F. Zhang, Y. T. Li and S. Y. Liu, *Macromolecules*, 2007, **40**, 9125-9132.

57 J. F. Lutz, O. Akdemir and A. Hoth, *J. Am. Chem. Soc.*, 2006, **128**, 13046-13047.

58 H. H. Xiao, R. G. Qi, S. Liu, X. L. Hu, T. C. Duan, Y. H. Zheng, Y. B. Huang and X. B. Jing, *Biomaterials*, 2011, **32**, 7732-7739.

59 S. Aryal, C. M. J. Hu and L. F. Zhang, *Acs Nano*, 2010, **4**, 251-258.

60 H. T. T. Duong, V. T. Huynh, P. de Souza and M. H. Stenzel, *Biomacromolecules*, 2010, **11**, 2290-2299.

61 Y. Z. Min, C. Q. Mao, S. M. Chen, G. L. Ma, J. Wang and Y. Z. Liu, *Angew. Chem., Int. Ed.*, 2012, **51**, 6742-6747.

62 J. Li, Y. Han, Q. Chen, H. Shi, S. u. Rehman, S. Mohammad, Z. Ge and S. Liu, *J. Mater. Chem. B*, 2014, DOI: 10.1039/C1033TB21383H.

63 T. S. Hauck, T. L. Jennings, T. Yatsenko, J. C. Kumaradas and W. C. W. Chan, *Adv. Mater.*, 2008, **20**, 3832-3838.

64 E. Engel, R. Schraml, T. Maisch, K. Kobuch, B. Koenig, R. M. Szeimies, J. Hillenkamp, W. Baumler and R. Vasold, *Invest Ophth Vis Sci*, 2008, **49**, 1777-1783.

For Table of Contents Graphical Abstract Use Only

Redox-responsive core cross-linked micelles based on cypate and cisplatin prodrugs-conjugated block copolymers for synergistic photothermal-chemotherapy of cancer

Yu Han, Junjie Li, Minghui Zan, Shizhong Luo, Zhishen Ge* and Shiyong Liu

Synergistic effect of photothermal and chemotherapy of cancers was demonstrated using redox-responsive core cross-linked micelles fabricated from cypate and cisplatin prodrugs-conjugated block copolymers.